Journal of Solid State Chemistry 181 (2008) 2165–2170

Contents lists available at ScienceDirect

Journal of Solid State Chemistry

journal homepage: www.elsevier.com/locate/jssc

# A sodium gadolinium phosphate with two different types of tunnel structure: Synthesis, crystal structure, and optical properties of $Na_3GdP_2O_8$

M. Fang, W.-D. Cheng *, H. Zhang, D. Zhao, W.-L. Zhang, S.-L. Yang

*Fujian Institute of Research on the Structure of Matter, State Key Laboratory of Structural Chemistry, The Graduate School of the Chinese Academy of Sciences, Fuzhou, Fujian 350002, China*

ARTICLE INFO

*Article history:*
Received 13 January 2008
Received in revised form
28 March 2008
Accepted 16 April 2008
Available online 3 May 2008

*Keywords:*
Crystal structure
Energy band
Phosphate
Optical properties

ABSTRACT

A sodium gadolinium phosphate crystal, $Na_3GdP_2O_8$, has been synthesized by a high-temperature solution reaction, and it exhibits a new structural family of the alkali-metal-rare-earth phosphate system. Although many compounds with formula $M_3LnP_2O_8$ have been reported, but they were shown to be orthorhombic [R. Salmon, C. Parent, M. Vlasse, G. LeFlem, Mater. Res. Bull. 13 (1978) 439] rather than monoclinic as shown in this paper. Single-crystal X-ray diffraction analysis shows the structure to be monoclinic with space group $C2/c$ and the cell parameters: $a = 27.55\,(25)$, $b = 5.312\,(4)$, $c = 13.935(11)$ Å, $\beta = 91.30(1)^\circ$, and $V = 2038.80$ Å$^3$, $Z = 4$. Its structure features a three-dimensional $GdP_2O_8^{3-}$ anionic framework with two different types of interesting tunnels at where Na atoms are located by different manners. The framework is constructed by Gd polyhedra and isolated $PO_4$ tetrahedra. It is different from the structure of $K_3NdP_2O_8$ [R. Salmon, C. Parent, M. Vlasse, G. LeFlem, Mater. Res. Bull. 13 (1978) 439] with space group $P2_1/m$ that shows only one type of tunnel. The emission spectrum and the absorption spectrum of the compound have been investigated. Additionally, the calculations of band structure, density of states, dielectric constants, and refractive indexes have been also performed with the density functional theory method. The obtained results tend to support the experimental data.



## 1. Introduction

Inorganic phosphates with a general formula $M_3Ln(PO_4)_2$ have been investigated in the past years due to their interesting optical properties [1–6], where M is a monovalent metal cation and Ln is a trivalent rare-earth cation, and these compounds contain a common basic structural unit of isolated $PO_4$ group. The common chemical features of these phosphates indicate that they are stable under normal conditions of temperature and humidity. Recently, our group reported compounds $LiGd_5P_2O_{13}$ which consists of isolated $PO_4$ tetrahedra linked with Ga polyhedra and $Li^+$ cations are located in the infinite tunnels, and $K_3Gd_5(PO_4)_6$ in which the structural units of Gd polyhedra and isolated $PO_4$ tetrahedra form a three-dimensional framework containing infinite tunnels in which the $K^+$ cations are located [7,8]. In addition, only several condensed polyphosphates containing Gd in ternary system have been reported [9–15]. For the type of $MGd(PO_3)_4$ compounds ($M$ = Na, K, Cs, and Ag), the basic structure units are helical ribbons $(PO_3)_n$ formed by corner-sharing $PO_4$ tetrahedra. The ribbons run along some directions of unit-cell with a period of four or eight tetrahedral. Theses chains are joined to each other by $GdO_8$ dodecahedra, giving a three-dimensional structure, with the $M^+$ cations located in framework tunnels [9–13]. The lattice of $LiGd(PO_3)_4$ is built of twisted zig-zag chains and make up of $PO_4$ tetrahedra sharing two corners, connected to the $GdO_8$ and $LiO_4$ polyhedra by common oxygen atoms to form a three-dimensional framework [14].

In view of the unusual compositional and structural diversity of phosphate compounds with gadolinium and they are potential applications in ultraviolet emission [7,8], magnetic [15], and nonlinear optical materials [16], we have continually designed and synthesized new compounds with fascinating properties in the system. In this paper, we will describe the synthesis, crystal structure, and optical properties of $Na_3GdP_2O_8$ by single-crystal X-ray diffraction (XRD), powder XRD, and absorption and emission spectra. In addition, we will investigate its electronic properties and carry out the calculations of crystal energy band, density of states (DOS), dielectric constants, and refractive indexes of $Na_3GdP_2O_8$ by the density functional theory (DFT) method.

## 2. Experimental

### 2.1. Synthesis of $Na_3GdP_2O_8$

Single crystals of $Na_3GdP_2O_8$ were grown by using a high-temperature solution reaction. Analytical reagents $Gd_2O_3$, NaCl, and $NH_4H_2PO_4$ were weighed in the molar ration of Na/Gd/

* Corresponding author. Fax: +86 591 371 4946.
*E-mail address:* cwd@ms.fjirsm.ac.cn (W.-D. Cheng).

0022-4596/$ - see front matter © 2008 Elsevier Inc. All rights reserved.
doi:10.1016/j.jssc.2008.04.013

P = 50:2:5, and the excess of NaCl and $NH_4H_2PO_4$ acted as a flux. These starting materials were finely ground in an agate mortar to ensure the best homogeneity and reactivity, then placed in a platinum crucible, and heated at 573 K for 4 h in order to decompose $NH_4H_2PO_4$. Afterward, the mixture was reground and heated to 1073 K for 24 h. Finally, the temperature was cooled to 873 K at a rate of 2 K/h and air-quenched to room temperature. A few colorless needle-shaped crystals were obtained from the melt of the mixture. After crystal structure determination, a polycrystalline sample of $Na_3GdP_2O_8$ was synthesized by solid-state reactions of stoichiometric amounts (Na/Gd/P = 3:1:2) of analytical reagent $NaCO_3$, $Gd_2O_3$, and $NH_4H_2PO_4$. The pulverous mixture was allowed to react at 1073 K for 100 h with several intermediate grindings in an opening Pt crucible. The purity nature of the sample was confirmed by powder XRD.

### 2.2. X-ray single crystal structure determination

A single crystal of $Na_3GdP_2O_8$ was selected for XRD determination. The diffraction data were collected on a Siemens SMART CCD diffractometer with graphite-monochromated Mo$K\alpha$ radiation (wavelength = 0.71073 Å) using the $\omega/2\theta$ scan mode at the temperature of 273 K. An empirical absorption correction was applied using SADABS program. The structure of the title compound was solved using direct methods and refined on $F^2$ by full-package [17]. Direct methods are used to solve a crystal structure and, therefore, to locate atoms of Gd. The remaining atoms were located in succeeding difference Fourier synthesis. Further details of the X-ray structural analysis are given in Table 1. The atomic coordinates and thermal parameters are listed in Table 2. Selected bond lengths and angles are given in Table 3. Residual peaks within −2.00/4.33 e/Å$^3$ remained near the Gd atom. This high residual electron density can be explained by the absorption correction performed by psi-scans for non-regular crystal shapes [18]. Further details of the crystal-structure investigations may be obtained from the Fachinformationzentrum Karlsruhe, 76344 Eggenstein-Leopoldshafen, Germany, on quoting the depository numbers CSD-418998 for this compound.

**Table 1**
Crystal data and structure refinement for $Na_3GdP_2O_8$

| | |
|---|---|
| Formula | $Na_9Gd_3P_6O_{24}$ |
| Formula weight (g/mol) | 1248.48 |
| Temperature (K) | 273(2) |
| Wavelength (Å) | 0.71073 |
| Crystal system | Monoclinic |
| Space group | $C2/c$ |
| Unit cell dimensions | $a = 27.55\ (2)$ Å |
| | $b = 5.312\ (4)$ Å |
| | $c = 13.935\ (11)$ Å |
| | $\beta = 91.299\ (13)$ |
| Volume, $Z$ | 2038.80(274) Å$^3$, 4 |
| $D_{calc}$ (g/cm$^3$) | 4.067 |
| Absorption coefficient | 10.433 |
| $\theta$ range (deg) | 3.25–27.49 |
| $F$ (000) | 2292 |
| Limiting indices | $-34 \leqslant h \leqslant 35; -6 \leqslant k \leqslant 6; -17 \leqslant l \leqslant 18$ |
| Reflections collected | 7447 |
| Independent reflections | 1791(Rint = 0.0407) |
| Refinement method | Full-matrix least-squares on $F^2$ |
| Absorption correction type | Multi-scan |
| GOF | 0.997 |
| Final $R$ indices [$I$>2sigma(I)] | 0.0407 |
| $R$ indices (all data) | 0.0654 |
| Largest diff. peak and hole (e/Å$^3$) | 4.33 and −2.00 |

**Table 2**
Atomic coordinates and equivalent isotropic displacement parameters for $Na_3GdP_2O_8$

| Atom | $x$ | $y$ | $z$ | $U^a_{eq}$ |
|---|---|---|---|---|
| Na(1) | 0.6184(1) | 1.0093(7) | 0.1369(3) | 0.0182(3) |
| Na(2) | 0.5545(1) | 1.5381(7) | 0.4199(3) | 0.0160(5) |
| Na(3) | 0.5000 | 0.0000 | 0.0000 | 0.0157(2) |
| Na(4) | 0.7211(1) | 0.9959(9) | 0.3228(3) | 0.0277(0) |
| Na(5) | 0.6516(1) | 0.4969(8) | 0.2663(3) | 0.0215(2) |
| Gd(1) | 0.5000 | 0.955(1) | 0.2500 | 0.0075(0) |
| Gd(2) | 0.6779(1) | 0.4893(1) | 0.0150(1) | 0.0075(1) |
| P(1) | 0.5581(1) | 0.5358(5) | 0.1524(2) | 0.0075(1) |
| P(2) | 0.6116(1) | 1.0132(5) | 0.3900(2) | 0.0076(2) |
| P(3) | 0.7709(1) | 0.5038(5) | −0.1041(2) | 0.0143(0) |
| O(12) | 0.5561(2) | 0.9932(11) | 0.3756(4) | 0.0098(1) |
| O(11) | 0.7177(2) | 0.4984(12) | −0.1365(4) | 0.0121(3) |
| O(10) | 0.6110(2) | 0.5315(12) | 0.1199(4) | 0.0145(2) |
| O(9) | 0.7976(2) | 0.2776(13) | −0.1449(4) | 0.0189(7) |
| O(8) | 0.5400(2) | 0.8100(11) | 0.1495(4) | 0.0094(3) |
| O(7) | 0.5252(2) | 0.3669(12) | 0.0897(4) | 0.0125(7) |
| O(6) | 0.7950(2) | 0.7421(14) | −0.1403(5) | 0.0265(5) |
| O(5) | 0.6382(2) | 0.9522(13) | 0.2990(4) | 0.0168(4) |
| O(4) | 0.6250(2) | 1.2803(12) | 0.4230(5) | 0.0180(9) |
| O(3) | 0.5569(2) | 0.4268(12) | 0.2540(4) | 0.0123(8) |
| O(2) | 0.6254(2) | 0.8267(12) | 0.4706(4) | 0.0154(1) |
| O(1) | 0.7726(3) | 0.4940(20) | 0.0057(5) | 0.0676(6) |

$U^a_{eq}$ is defined as one-third of the trace of the orthogonalized $U_{ij}$ tensor.

**Table 3**
Selected bond distances (Å) and angles (deg) for $Na_3GdP_2O_8$

| | | | |
|---|---|---|---|
| Na1–O5 | 2.331(7) | Na1–O8 | 2.415(7) |
| Na1–O2$^{i}$ | 2.487(7) | Gd2–O4$^{i}$ | 2.276(6) |
| Na1–O10 | 2.557(8) | Gd2–O2$^{vii}$ | 2.292(6) |
| Na1–O9$^{ii}$ | 2.577(8) | Gd2–O6$^{ii}$ | 2.363(6) |
| Na1–O6$^{ii}$ | 2.734(8) | Gd2–O9$^{xv}$ | 2.386(6) |
| Na1–O10$^{iii}$ | 2.791(8) | Gd2–O10 | 2.390(6) |
| Gd2–O11 | 2.401(6) | Gd2–O1 | 2.614(8) |
| Gd2–O1$^{xv}$ | 2.927(10) | Na2–O4 | 2.377(7) |
| Na2–O7$^{iv}$ | 2.378(7) | Na2–O3$^{iii}$ | 2.388(7) |
| P1–O3 | 1.532(6) | Na2–O12$^{iii}$ | 2.496(7) |
| P1–O7 | 1.534(6) | Na2–O7$^{v}$ | 2.568(7) |
| P1–O10 | 1.535(6) | Na2–O2$^{iii}$ | 2.570(7) |
| P1–O8 | 1.540(6) | Na2–O12 | 2.960(7) |
| P2–O5 | 1.514(6) | P2–O4 | 1.534(7) |
| P2–O2 | 1.539(6) | Na3–O12$^{vii}$ | 2.349(6) |
| P2–O12 | 1.542(6) | Na3–O12$^{viii}$ | 2.349(6) |
| Na3–O7 | 2.409(6) | Na3–O7$^{ix}$ | 2.409(6) |
| Na3–O8$^{x}$ | 2.543(6) | P3–O6 | 1.521(7) |
| Na3–O8$^{xi}$ | 2.543(6) | P3–O11 | 1.525(6) |
| P3–O9 | 1.525(7) | P3–O1 | 1.530(8) |
| Na4–O5 | 2.313(7) | Na4–O1$^{xiii}$ | 2.393(9) |
| Na4–O6$^{v}$ | 2.510(9) | Na4–O9$^{xiv}$ | 2.591(8) |
| Na4–O11$^{xiv}$ | 2.688(8) | Na4–O11$^{v}$ | 2.748(8) |
| Na4–O9$^{ii}$ | 2.792(7) | Na4–O6$^{ii}$ | 2.865(8) |
| Na5–O11$^{xiv}$ | 2.244(7) | Na5–O10 | 2.313(7) |
| Gd1–O8$^{viii}$ | 2.355(6) | Gd1–O3 | 2.356(6) |
| Gd1–O3$^{xvi}$ | 2.56(6) | Gd1–O12$^{viii}$ | 2.371(6) |
| Gd1–O12$^{xi}$ | 2.71(6) | Gd1–O7$^{xvi}$ | 2.760(6) |
| O5–Na1–O8 | 93.6(2) | O8$^{viii}$–Gd1–P1 | 168.89(15) |
| O5–Na1–O2$^{i}$ | 158.0(3) | O3–Gd1–P1 | 27.65(15) |
| O8–Na1–O2$^{i}$ | 108.0(2) | O3$^{xvi}$–Gd1–P1 | 77.29(16) |
| O3–P1–O7 | 106.3(4) | O3–P1–O10 | 108.0(4) |
| O7–P1–O10 | 112.1(3) | O3–P1–O8 | 111.6(3) |
| O7–P1–O8 | 110.6(4) | O10–P1–O8 | 108.4(3) |
| O5–P2–O4 | 109.3(4) | O5–P2–O2 | 110.9(4) |
| O4–P2–O2 | 108.8(4) | O5–P2–O12 | 111.9(3) |
| O4–P2–O12 | 109.6(3) | O2–P2–O12 | 106.2(3) |

Symmetry codes: (1) $x,-y+2,z-1/2$ (2) $-x+3/2,-y+3/2,-z$ (3) $x,y+1,z$ (4) $-x+1,y+1,-z+1/2$ (5) $x,-y+2,z+1/2$ (6) $-x+1,y+2,-z+1/2$ (7) $x,-y+1,z-1/2$ (8) $-x+1,y-1,-z+1/2$ (9) $-x+1,-y,-z$ (10) $-x+1,-y+1,-z$ (11) $x,y-1,z$ (12) $-x+1,y-2,-z+1/2$ (13) $-x+3/2,y+1/2,-z+1/2$ (14) $x,-y+1,z+1/2$ (15) $-x+3/2,-y+1/2,-z$ (16) $-x+1,y,-z+1/2$ (17) $-x+3/2,y-1/2,-z+1/2$.

### 2.3. Spectral and powder X-ray measurements

The samples used for spectral measurements were polycrystalline powder synthesized by solid-state reactions. To give evidence that it contains pure phase of sample, we determined the powder XRD pattern of $Na_3GdP_2O_8$ using RIGAKU DMAX2500 diffractometer with Cu$K\alpha$ radiation (step size of 0.05° and range $2\theta = 10$–80°). The Rietveld refinement [19,20] was carried out with the Rietica program [21]. Fig. 1 gives the powder XRD pattern of $Na_3GdP_2O_8$, which compares with the simulated one, confirming the monophasic nature of the prepared samples. The absorption spectrum was recorded on a cary-500 UV/vis/NIR spectrophotometer in the wavelength range of 200–700 nm. The emission spectrum was measured on an FL/FS 900 time-resolved fluorescence spectrometer using Xe lamp at room temperature.

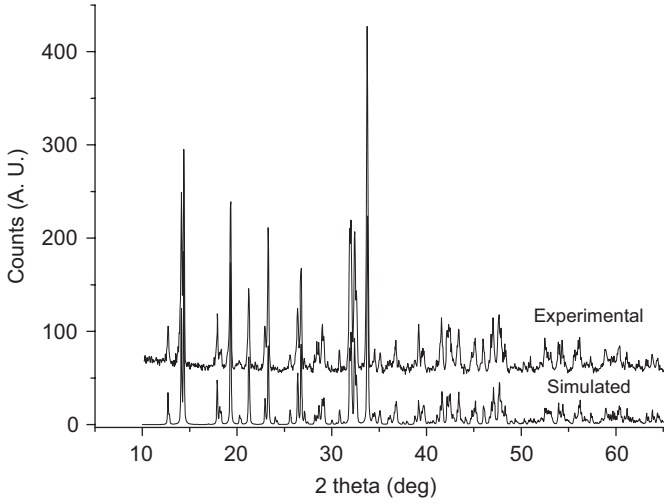


**Fig. 1.** Simulated and experimental powder X-ray (Cu$K\alpha$) diffraction pattern for $Na_3GdP_2O_8$.

### 2.4. Computational descriptions

The crystallographic data of the solid-state compound $Na_3GdP_2O_8$ by single-crystal XRD were used to calculate the electronic band structure of this compound. The calculations of electronic band structures were performed at the DFT level using one of the three non-local gradient-corrected exchange-correlation functionals (GGA-PBE) and running on the CASTEP code [22,23], which uses a plane wave basis set for the valence electrons and norm-conserving pseudopotential for the core states. The number of plane waves included in the basis was determined by a cutoff energy, $E_c$ of 450 eV. Pseudoatomic calculations were performed for O ($2s^2 2p^4$), P ($3s^2 3p^3$), Na ($3s^1$), Gd ($4f^7 5d^1 6s^2$). The calculating parameters and convergent criteria were set by the default values of CASTEP code [24]. The calculations of linear optical properties described in terms of complex dielectric function $\varepsilon(\omega) = \varepsilon_1(\omega) + i\varepsilon_2(\omega)$ were also carried out in this work. The imaginary part $\varepsilon_2(\omega)$ can be thought of as detailing the real transitions between occupied and unoccupied electronic states. The real and imaginary parts were linked by a Kramers–Kroning transform. This transform was used to obtain the real part $\varepsilon_1(\omega)$ of the dielectric function.

## 3. Results and discussions

### 3.1. Crystal structure

Crystallographic analysis reveals that the $Na_3GdP_2O_8$ compound belongs to the monoclinic system with space group $C2/c$. The structural units of $Na_3GdP_2O_8$ are Gd polyhedra and isolated $PO_4$ tetrahedra, forming a three-dimensional $GdP_2O_8^{3-}$ anionic framework containing two types of different infinite tunnels along the b axis in which the Na atoms are located, as shown in Fig. 2. Fig. 3(a) shows one type of tunnel, it is constructed by 8-sided windows running along with the $b$-axis, and each of the windows is formed by the edges of four $GdO_8$ or $GdO_7$ polyhedra and four $PO_4$ tetrahedra. In this tunnel, three chains those are formed by Na

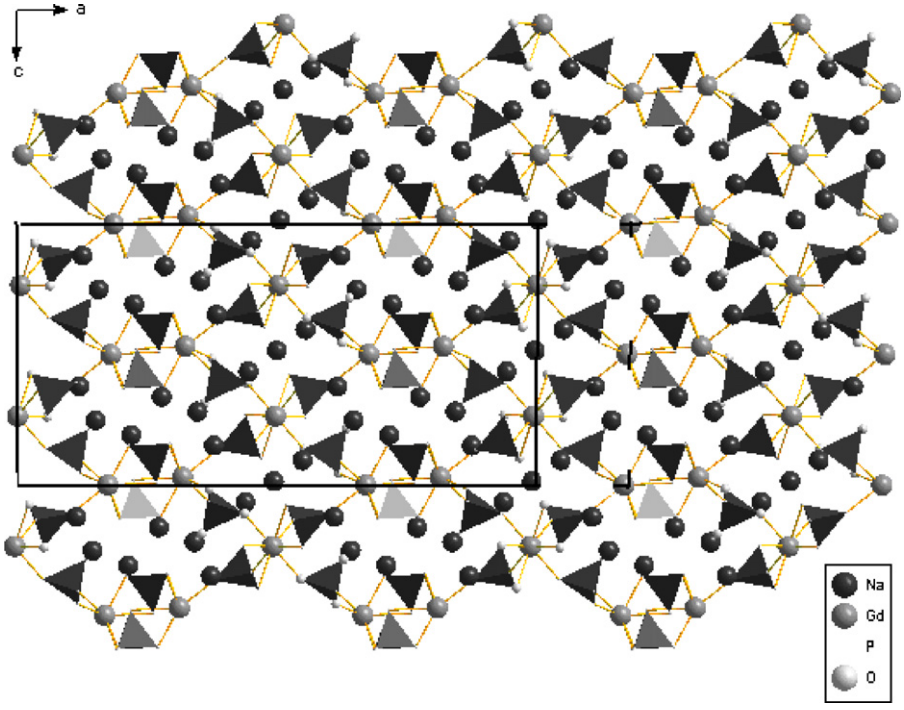


**Fig. 2.** Projection of the structure of $Na_3GdP_2O_8$ with a unit cell edge along the $b$-axis. The Na–O bonds are omitted for clarity.

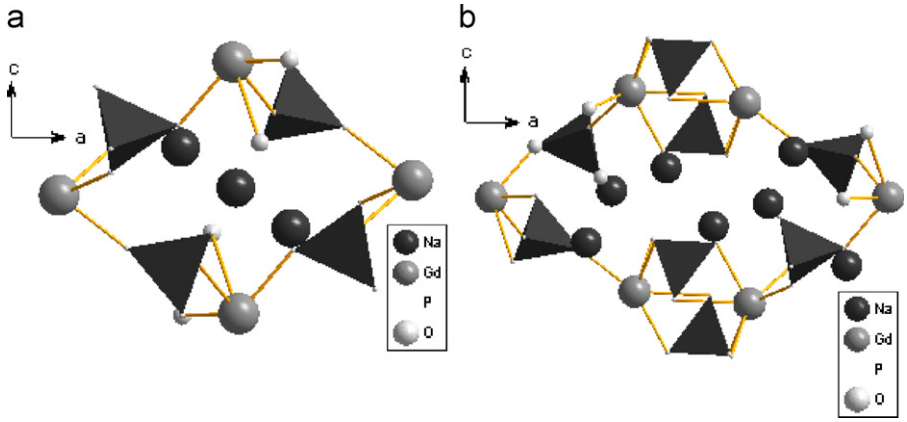


**Fig. 3.** Two types of different infinite tunnels along the *b*-axis.

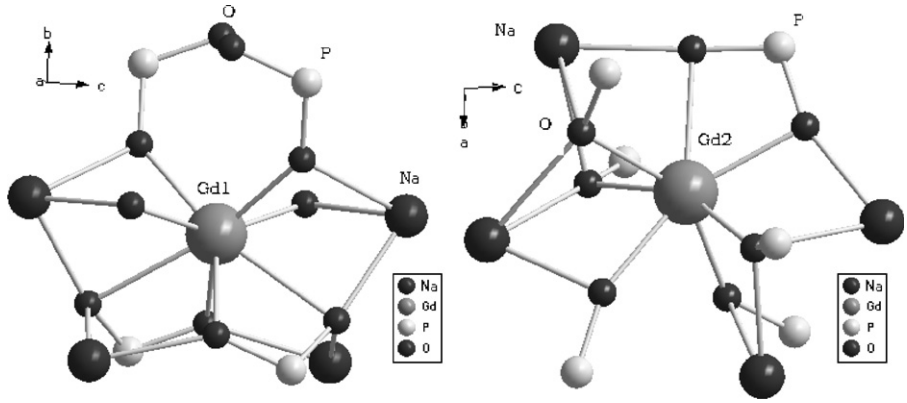


**Fig. 4.** The coordinated environment of the Gd1 and Gd2 atoms.

atoms along b axis arrange in a line on the ac plane. Fig. 3(b) shows the other type of tunnel, it is made up of six [GdO] polyhedra linked with six $PO_4$ tetrahedra. And in this tunnel, six chains those are formed by Na atoms along the *b*-axis arrange in a circle on the ac plane. Moreover, the latter type of tunnel is not existed in the structure of $K_3NdP_2O_8$ [25].

Fig. 4 shows the Gd coordination environment in $Na_3GdP_2O_8$ compound. Gd1 is surrounded by eight O atoms, whereas Gd2 is coordinated by seven O atoms. All the Gd–O bond distances are consistent with those reported previously [26]. All the Gd polyhedra are greatly distorted. Each Gd1 polyhedron is edge-shared with two Na–O polyhedra, and face-shared with two Na–O polyhedra. Each Gd2 polyhedron is edge-shared with three Na–O polyhedra, and face-shared with one Na–O polyhedra. All the Gd polyhedra are also linked with isolated $PO_4$ tetrahedra via sharing O atoms, resulting in a three-dimensional $GdP_2O_8^{3-}$ anionic framework.

The P–O bond distances vary from 1.514(4) to 1.530 Å, and O–P–O angles range from 106.2(3) TO 112.1(3)°. This indicates that $PO_4$ tetrahedras are slightly distorted. These $PO_4$ tetrahedras are isolated from each other because they only share O atoms with Gd polyhedra to form a three dimensional $GdP_2O_8^{3-}$ anionic framework.

### 3.2. Band structure and DOS

The energy band structures and DOS of $Na_3GdP_2O_8$ were calculated by density functional methods. The calculated band structure of $Na_3GdP_2O_8$ is shown in Fig. 5. In order to assign these bands, the total density of states (TDOS) and partial DOS (PDOS) are shown in Fig. 6.

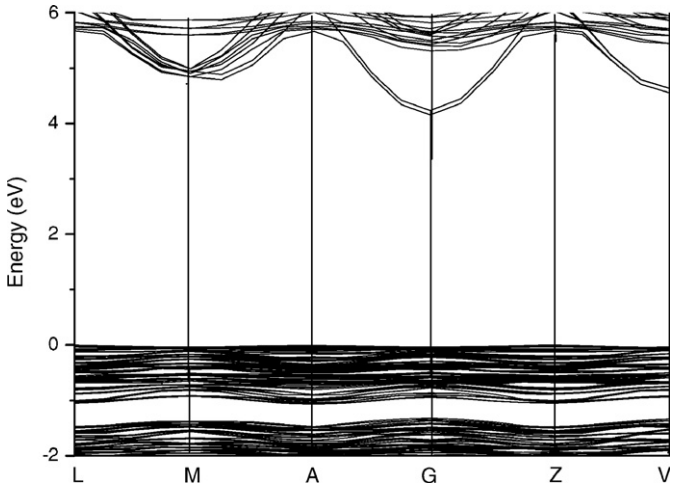


**Fig. 5.** Calculated energy band structure of $Na_3GdP_2O_8$.

As shown in Fig. 5, the lowest point of the CBs is localized at the G point and has energy of 4.15 eV while the highest energy of the valance bands (VBs) is taken as the reference, hereafter. The energy at the G point of the VBs is −0.035 eV. Accordingly, it is reasonable to consider $Na_3GdP_2O_8$ as an insulator with an indirect band gap of around 4.185 eV. According to Fig. 6, the O–2*p* states make main contributions to the top of the VBs near the Fermi

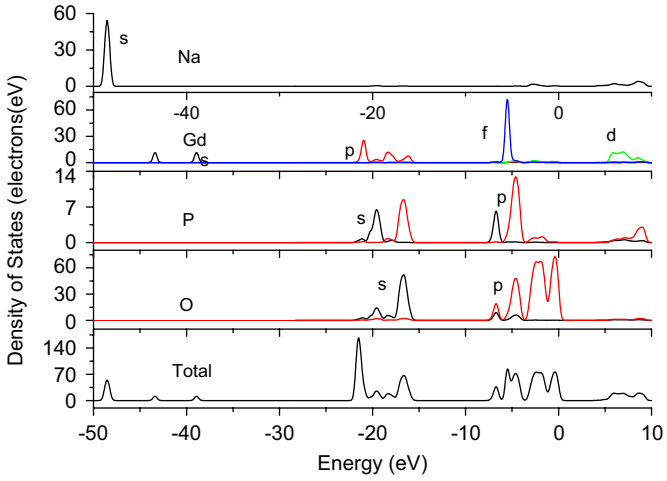


**Fig. 6.** TDOS and PDOS of $Na_3GdP_2O_8$.

level, and the Gd–6*s* states result in the VBs near −43.3 and −38.8 eV. The VBs near −5.36 eV are mostly formed by the Gd–4*f* states with the mixings of the O–2*p*, P–3*p* states, and the VBs near −7.58 eV are derived from the O–2*p* with a small mixing of P–3*s* states. The VBs from −22.1 to −15.3 eV are constructed by the mixings of the Gd–5*p*, O–2*s*, P–3*s*, and P–3*p* states. The bands from the bottom of the CBs to 10.0 eV result from the unoccupied Gd–5*d* states with the mixings of the P–3*p* states.

### 3.3. Optical properties

Fig. 7a illustrates the absorption spectra of $Na_3GdP_2O_8$. The strongest peak is located at 208 nm. And the absorption edge is observed at wavelengths of 230 nm (5.4 eV). In view of Fig. 6 about TDOS and PDOS plots, we can identify that the absorption band mostly originates from charge transfers from O–2*p* state to Gd–5*d* state. The emission peaks of the title compound are observed at wavelengths of 420 nm from the emission spectrum under the excitation at 330 nm (Fig. 7b).

In addition, we examined the linear optical response properties of $Na_3GdP_2O_8$. We calculated the imaginary part $\varepsilon_2(\omega)$ and the real part $\varepsilon_1(\omega)$ of the frequency-dependent dielectric function without the DFT scissor operator approximation and with that of the shift energy of 1.20 eV (calculated lowest VB–CB transition energy 4.2 eV and experimental value 5.4 eV, respectively). The reason for this situation is that the GGA cannot accurately describe the eigenvalues of the electronic states, which causes quantitative underestimation of band gaps [27]. The refractive index is linked with the dielectric constant by the relation of $n^2(\omega) = \varepsilon(\omega)$. The calculated dielectric constants of static case $\varepsilon(0)$ and the refractive indexes $n$ at 1064 nm in $x$, $y$, and $z$ directions are listed in Table 4. It is found that the calculated results with the shift energy of 1.20 eV are a little smaller than those without the DFT scissor operator approximation. Since the refractive indexes $Na_3GdP_2O_8$ have not been measured and reported, we compare the calculated results with the observed refractive indexes of the other phosphate crystals, which are generally ranging from 1.40 to 1.60 [28]. Accordingly, our calculated refractive indexes well fall in this range. Fig. 8 displays calculated real and imaginary parts of dielectric functions of $Na_3GdP_2O_8$ in different polarization directions without the DFT scissor operator approximation. The part $\varepsilon_2(\omega)$ can be used to describe the real transitions between the occupied and the unoccupied electronic states. There is a strong absorption peak around 8.75 eV, and the absorption edge is localized about 5.1 eV, which corresponds to that 5.4 eV of the

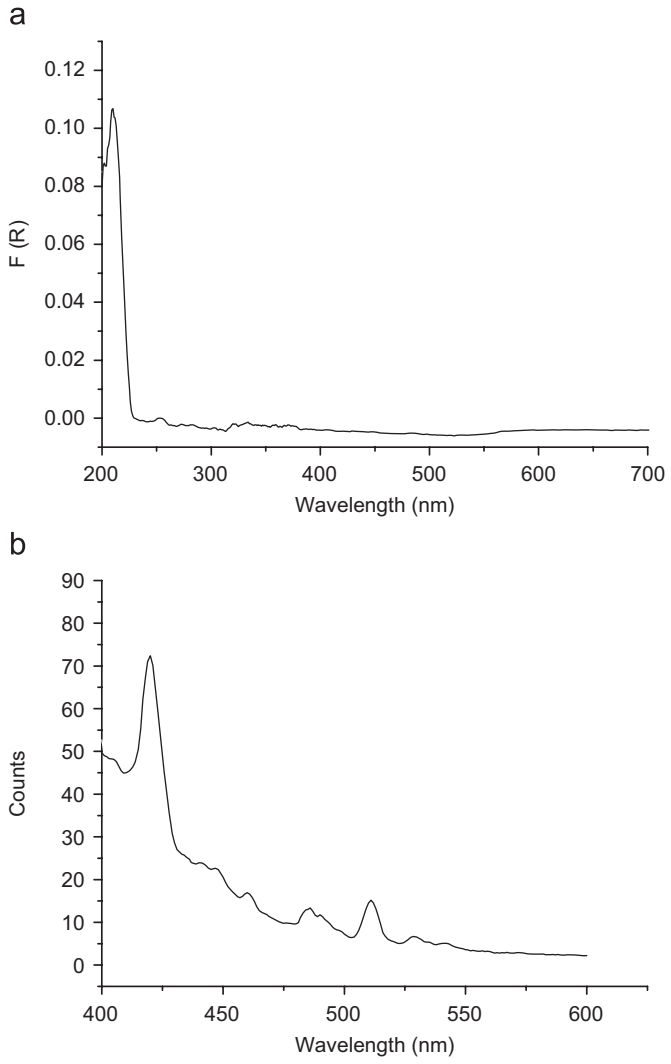


**Fig. 7.** Absorption (a) and emission (b) spectra of $Na_3GdP_2O_8$.

**Table 4**
Calculated dielectric constants of static case and refractive indexes at 1064 nm in different polarization directions

| Scissor operator | | | | | | |
|---|---|---|---|---|---|---|
| (eV) | $\varepsilon_x(0)$ | $\varepsilon_y(0)$ | $\varepsilon_z(0)$ | $n_x$ | $n_y$ | $n_z$ |
| 0 | 2.6527 | 2.7085 | 2.5999 | 1.6287 | 1.6458 | 1.6124 |
| 1.20 | 2.4675 | 2.5143 | 2.4248 | 1.5708 | 1.5857 | 1.5572 |

experimental spectra (Fig. 7a). According to Fig. 6, these peaks are assigned as the electronic transitions from the O–2*p* to the Gd–5*d* states.

## 4. Conclusions

In this work, a new sodium gadolinium phosphate with two different types of tunnels structure, $Na_3GdP_2O_8$, as been grown by a high-temperature solution reaction. It crystallizes in the monoclinic system with space group *C*/2*c* and is composed of $GdP_2O_8^{3-}$ anionic framework containing two different types of infinite channels along the *b*-axis in which the Na atoms are located according to different manner. The spectral measurements and analyses indicate that the strongest absorption peak is

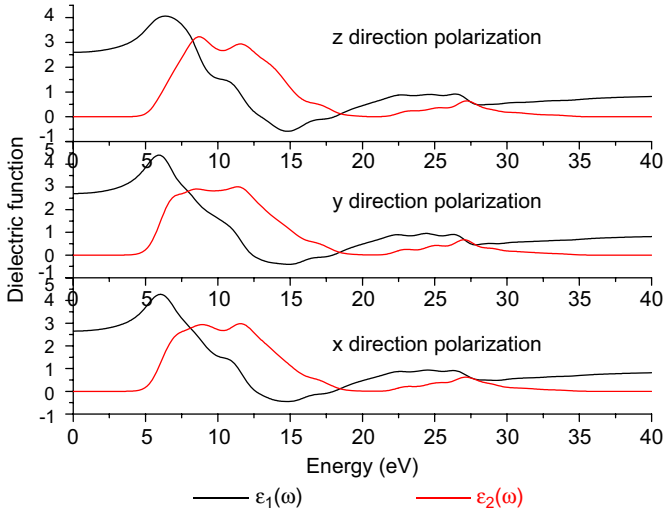


**Fig. 8.** Calculated real and imaginary parts of the dielectric functions in different polarization directions for $Na_3GdP_2O_8$.

localized about 208 nm and assigned as electron transition from O–2*p* state to G–5*d* state. Both the experimental spectrum and the calculated band structure show that $Na_3GdP_2O_8$ possesses the insulating feature with a width of band gap. The top of the VBs originates from the O–2*p* states, and the bottom of the CBs results from the Gd–5*d* states. Additionally, dielectric constants and refractive indexes of $Na_3GdP_2O_8$ are calculated and the estimated results well fall in the range of the phosphate experimental data.

## Acknowledgments

This investigation was based on work supported by the National Natural Science Foundation of China under projects 20373073 and the National Basic Research Program of China (no. 2007CB815307), the Funds of Chinese Academy of Sciences (KJCX2-YW-H01), and Fujian Key Laboratory of Nanomaterials (no. 2006L2005).

## Appendix A. Supplementary materials

Supplementary data associated with this article can be found in the online version at doi:10.1016/j.jssc.2008.04.013.

## References

[1] M. Kloss, B. Finke, L. Schwarz, D. Haberland, J. Lumin. 72–74 (1997) 684–686.
[2] M. Kloss, L. Schwarz, J.P.K. HÖlsä, Acta Phys. Pol. A 95 (1999) 343–349.
[3] V.A. Morozoc, A.P. Bobylev, N.v. Gerasimova, A.N. Kirichenko, V.V. Mikhailin, G. Ya. Pushkina, B.I. Lazoryak, L.N. Komissarova, Russ. J. Inorg. Chem. 46 (2001) 711–718.
[4] L. Benarafa, L. Rghioui, R. Neffar, M. Saidi Idrissi, M. Knidiri, A. Lorriaux, F. Wallart, Spectrochim. Acta A 61 (2005) 419–430.
[5] L. Schwarz, M. Kloss, A. Rohmann, U. Sasum, D. Haberland, J. Alloys Compds. 275–277 (1998) 93–95.
[6] J. Zan Letho, P. Houenou, R.C.R. Eholie, Acad. Sci. (Pairs) Ser. П 307 (1988) 1177–1179.
[7] Jing Zhu, Wen-Dan Cheng, Dong-Sheng Wu, Hao Zhang, Ya-Jing Gong, Hua-Nan Tong, Dan Zhao, Inorg. Chem. 46 (2007) 208–212.
[8] Jing Zhu, Wen-Dan Cheng, Dong-Sheng Wu, Hao Zhang, Ya-Jing Gong, Hua-Nan Tong, Dan Zhao, Cryst. Growth Des. 6 (2006) 1649–1652.
[9] J. Amami, M. Férid, M. Trabelsi-Ayedi, Mater. Res. Bull. 40 (2005) 2144–2152.
[10] Walid Rekik, Houcine NaÕÈli, Tahar Mhiri, Acta Crystallogr. C 60 (2004) i50–i52.
[11] H. Ettis, H. Naili, T. Mhiri, Cryst. Growth Des. 3 (2003) 599–602.
[12] H. Naıli, T. Mhiri, Acta Crystallogr. E 61 (2005) i204–i207.
[13] Houcine Näili, Hasna Ettis, Tahar Mhiri, J. Alloys Compds. 424 (2006) 400–407.
[14] Hasna Ettis, Houcine Naili, Tahar Mhiri, J. Solid State Chem. 179 (2006) 3107–3113.
[15] H. Ettis, H. Naili, T. Mhiri, Mater. Chem. Phys. 102 (2007) 275–280.
[16] I. Parreu, J.J. Carvajal, X. Solans, F. Díaz, M. Aguilo, Chem. Mater. 18 (2006) 221.
[17] G.M. Sheldrick, SHELXTL-97 Program for Refining Crystal Structure, University of Göttingen, Göttingen, Germany, 1997.
[18] C. Kremer, Inorg. Chim. Acta 294 (1999) 47–55.
[19] H.M. Rietveld, Acta Crystallogr. 22 (1967) 151.
[20] H.M. Rietveld, Acta Crystallogr. 25 (1969) 589.
[21] B.A. Hunter, Lhpm-rietica, 〈www.rietica.Org〉.
[22] M. Segall, P. Linda, M. Probert, C. Pickard, P. Hasnip, S. Clark, M. Payne, Materials Studio CASTEP, Version 2.2, 2002.
[23] M. Segall, P. Linda, M. Probert, C. Pickard, P. Hasnip, S. Clark, M. Payne, J. Phys.: Condens. Mater. 14 (2002) 2717–2744.
[24] J.R. Macdonald, M.K. Brachman, Rev. Mod. Phys. 28 (1956) 383.
[25] R. Salmon, C. Parent, M. Vlasse, G. LeFlem, Mater. Res. Bull. 13 (1978) 439.
[26] M.I. Ogden, B.W. Skelton, A.H. White, CR. Chim. 8 (2005) 181.
[27] R. Terki, G. Bertrand, H. Aourag, Microelectron. Eng. 81 (2005) 514.
[28] J.A. Dean (Ed.), Lange's Handbook of Chemistry, thirteenth ed, McGraw-Hill, New York, 1985.